Identification of ATP2C1 mutations in the patients of Hailey-Hailey disease

xiaoli li
  Xi'an Jiaotong University

dingwei zhang
  Xi'an Jiaotong University

jiahui ding
  Xi'an Jiaotong University

li li
  Xi'an Jiaotong University

zhenghui wang
  Xi'an Jiaotong University

Research article

Keywords: Familial benign chronic pemphigus, ATP2C1, gene mutation, p63

Abstract

Background: Familial benign chronic pemphigus (OMIM 169600), also known as Hailey-Hailey disease (HHD), is a clinically rare bullous Dermatosis. However the mechanism has not been clarified.

Objective: To detect novel mutations in exons of ATP2C1 gene in HHD patients; to explore the mechnism of HHD pathogenesis by examining the expression profile of hSPCA1, Mir-203, p63, Notch1 and HK⬚ proteins in the skin lesions of HHD patients.

Methods: Genomic DNA was extracted from peripheral blood of HHD patients. All exons of ATP2C1 gene in HHD patients were amplified by PCR and the products were purified and sequenced. All related signaling proteins of interest were stained by using skin lesion tissues from HHD patients and Mir-203 levels were also determined. Results: In this study, one synonymous mutation c.G2598A (in exon 26), one nonsense mutation c.C635A and two missense mutations c.C1286A (p.A429D) and c. A1931G (p. D644G) were identified. The nonsense mutation changed codon UCG to stop codon UAG, causing a premature polypeptide chain of the functional region A. The two missense mutations were located in the region P (phosphorylation region) and the Mn binding site of hSPCA1. The calcium pump was not no longer functional due to impaired protein structures. The level of hSPCA1 was significantly decreased in HHD patients compared to the normal human controls, accompanied by an increase of Mir-203 level and a decrease of p63 and HK⬚ levels.

Conclusion: In HHD patients, these factors may be involved in the signaling pathways of HHD pathogenesis. In addition, Notch1, which was negatively regulated p63, is downregulated. Our data showed that both p63 and Mir-203 may have significant regulatory effects on Notch1 in the skin.

Background

Familial benign chronic pemphigus (OMIM 169600), also known as Hailey-Hailey disease (HHD), is a clinically rare bullous Dermatosis, and mainly manifested as erosion, erythema, accompanied with blisters and pimples. The incidence of this disease is approximately 0.002% [1], and has no significant difference between men and women [2]. Gu Heng et al reported that HHD had higher incidence in men than in women, but more supporting evidence are needed. HHD is currently not curable, and symptomatic treatment is the main strategy taken so far to reduce symptoms and prevent disease recurrence[3]. Treatment methods include systemic therapy, physical therapy, topical drugs and surgery. Conventional treatments include using humectants to protect the skin barrier, using antifungals, antibiotics, and antivirals to prevent infections[4–6], using cortisol to reduce inflammation, and using topical vitaminsto promote the differentiation of epidermal keratinocytes and regulate intercellular Ca^{2+} concentrations[7–9]. Patients can use drugs such as cyclosporin, methotrexate, dapsone, and type A botulinum toxin if they fail to have satisfactory outcome with conventional treatment[10]. Other therapies include combination therapy (prednisone, dapsone, tripterygium, and antibiotics), reported by Gu Heng et al., have great onset rate and efficacy in treating patients with severe HHD. However, we need to further revaluate the long-term

efficacy of combination therapy. Biopharmaceutical is the focus of drug development in the future, and has shown satisfactory clinical efficacy in a variety of skin diseases[11].

HHD is caused by mutations in the ATP2C1 gene. ATP2C1 is expressed in the skin as well as the brain, skeletal muscle, placenta, heart, and lungs. In humans, ATP2C1 mutations rarely cause skin tumors, squamous cell carcinoma and basal cell carcinomain HHD lesions[12–15]. Liver failure with HHD was ever reported. There are also some cases that have emotional disorders or have no desire in almost all activities. It is believed that HHD development is due to insufficient gene dose of ATP2C1. The protein level of hSPCA1 (the human secretory pathway Ca^{2+}/Mn^{2+}-ATPase protein 1, hSPCA1) encoded by the ATP2C1 in the Golgi apparatus is strikingly decreased, resulting in an increase in the intracellular Ca^{2+} concentration. As an important messenger, Ca^{2+} has siginificant impact on the maturation and differentiation of keratinocytes. Increased Ca^{2+} concentration eventually destroy cell-to-cell connections.

Mir-203 is a family member of tumor suppressor genes. It is a type of short, non-coding single-stranded miRNA. Mir-203 binds to the 3′ untranslated region of the target gene mRNA and induces post-translational silence[16]. Recently, researchers found that numberous miRNAs including Mir-203 play important roles in tumorigenesis and development. Mir-203 is abberantly expressed in many type of tumors, such as lung cancer, breast cancer, and squamous cell carcinoma. Mir-203 has the highest abundance in the skin, and is exclusively expressed in keratinocytes, indicating that it may be a key to various biological functions of keratinocytes [17]. When keratinocytes treated with high concentration of Ca^{2+}, Mir-203 was upregulated > 3-fold[17, 18].

The transcription factor p63 is a member of the p53 tumor suppressor family and plays an important role in the regulation of epidermal growth, keratinocyte differentiation[19], cell adhesion and cell migration[20]. During keratinization, the expression level of ATP2C1 is strikingly decreased, so does p63. Numerous studies have shown that p63 regulates downstream target genes and also plays roles in a variety of intracellular signaling pathways [21, 22]. p63 and Notch1, two important factors that regulate cell proliferation and differentiation, cell adhesion and other functions in keratinocytes, are negatively regulated to each other[19]. Mature Mir-203 binds to p63 3'-UTR and downregulate p63[23]. In animal experiments, Mir-203 affected the "stemness" of mouse skin stem cells by targeting p63 expression, thus enhancing the differentiation capacity of basal cells [24, 25]. Mir-203 can also inhibit Notch1 expression by downregulating ligand Jagged1 in the Notch1 pathway [26, 27].

Hexokinase is a key enzyme in the first step of glycolytic pathway, catalyzing glucose into glucose 6-phosphate[28]. In human cells, hexokinase has four subtypes (I-IV), of which HKⅡ is the one present in human keratinocytes and regulates metabolism of glucose and lactate. Therefore, inhibiting HKII activity can effectively block sugar metabolism. HKⅡ gene is a target gene of p63, and p63 downregulation can reduce 80% of HKⅡ mRNA. In keratinocytes, the p63-HKⅡ axis is an important pathway regulating cell metabolism and proliferation. Downregulation of HKⅡ decreased ATP production, which in turn further compromized hSPCA1 function that is greatly dependent on energy supply.

In this study, we search for novel mutations of ATP2C1 by sequencing the gene from 2 different HHD pedigrees and 2 sporadic cases. We analyzed the impact of these mutations on the structure and function of hSPCA1 by using bioinformatics tool. We also examined the expression levels of hSPCA1, Mir-203, p63, Notch1, and HK⬚ in the skin lesion tissues of HHD patients. Whether the expression changes of these proteins are causative to the pathogenesis of HHD, needs further investigation.

Methods

Patients

The study subjects were HHD patients enrolled in the dermatology clinic of the Second Affiliated Hospital of Xi'an Jiaotong University, and pathological biopsy was performed on the patient's typical skin lesions to further confirm the diagnosis. The samples from 2 patients in pedigree I, II and 2 sporadic patients were collected. The patient's information such as gender, age, and skin lesion performance, time of onset, and family history was collected.

HE staining

Tissues were selected from a typical site of the patient's skin lesions following a biopsy under local anesthesia. The removed tissues were placed in 4% formaldehyde solution and fixed at 4 °C for >4 hours; the tissues were then rinsed under water for 10 minutes and then dehydrated in a biological tissue dehydrator following standard procedures. The tissues were then immediately put into 60 °C paraffin, and poured into the embedding box. After the paraffin is completely cooled down, the tissue was sectioned with thickness of 5 μm. The tissue sections were deparaffined following to standard procedures. The dewaxed sections were then stained in the following order: hematoxylin solution for 5 min; tap water for 2 min; 75% hydrochloric acid ethanol for 10 min; tap water for 5 min; ammonia water pan-blue for 15 s; tap water for 1 min; acidified eosin ethanol solution 1.5 min; tap water for 1min. Dehydration and transparentization were performed in the following order: 95% ethanol (I) 1 min; 95% ethanol (II) 1 min; anhydrous ethanol (I) 1 min; anhydrous ethanol (II) 1 min; xylene (I) 1 min; xylene (⬚) 5 min. Neutral gum was added to seal the slides, covered with a cover glass, and then placed under an upright microscope for imaging.

DNA extraction

2 ml of peripheral venous blood were drawn from 2 patients with HHD from two different pedigrees and 2 sporadic patients following to the patient's consent. As controls, 2 ml of peripheral blood were collected from the patient's healthy family members and 100 normal people who were not blood related. The blood was collected in a 2% EDTA anticoagulant tube. The DNA was immediately extracted or stored in a -20 °C refrigerator. DNA extraction from peripheral blood was performed according to the following protocols: 200 μl of proteinase K solution was added to 200 μl of fresh or thawed blood and mixed well, and then 200 μl of binding solution was added and mixed thoroughly by vortexing, and incubated at 70 °C for 10 minutes; 100 μl of isopropanol was added after the samples cooled down, vortexed immediately to mix thoroughly, and then put it into the AC column, centrifuged at 13,000 rpm for 60 seconds, and then discarded the flow-through in the collection tube; the inhibitor remover IR and the rinse solution WB were

added sequentially, centrifuged at 12,000 rpm for 30 seconds and discarded the flow-through. 100 μl of pre-warmed elution buffer EB was added onto the center of the adsorption membrane, and then centrifuged at 12,000 rpm to collect DNA solution; the DNA product was stored at 4 °C, or at -20 °C for long-term use.

ATP2C1 primers and PCR reactions

Primer sequences were designed and verified using Primer Permier 5.0. All upstream and downstream primers cover some intron sequences on both sides of the exon. Primer synthesis and purification of PCR product were completed by Beijing Aoke Dingsheng Biotechnology Co., Ltd. PCR reaction: 2 × Taq Master MIX, 25 μl; DNA template, 5 μl; forward primer, 1 μl; reverse primer 1 μl; double distilled water, 18 μl; total volume, 50 μl. PCR protocol was summarized in Table 1. Protocol I was used for exon 1, protocol III was used for exon 5, 7, 12, 27 and 28 and protocol II was used for other exons.

Analysis of sequencing results

The sequencing data of each exon was read by Chromas 2.4 and aligned with the original sequence of human *ATP2C1* gene. Mutations found in alignment were compared with those previously reported. The mutation was considered to be novel if it was not previously reported.

IHC staining

The skin tissues collected from patients with HHD were cut into thickness of 4-5 μm by using a paraffin microtome. The sections were deparaffined and rehydrated following to standard procedures. Hydrogen peroxide (0.3%) was added onto the sections to block endogenous peroxidase, followed by 3 times of PBS wash, 5 ~ 10 min each time. The sections were then incubated with 0.1% saponin for 30 min, followed by PBS wash; 10% normal goat serum was added onto the sections and incubated at 37 °C for 30 min to cover non-specific sites; the blocking serum was then discarded and the primary antibody (hSPCA1, p63, Notch1, HK⍰; 1:50 dilution) was added and incubated at 4 °C for 24 ~ 72 hours; the sections were then washed with PBS for 3 times, 5~10 min each time; secondary antibodies (goat anti-rabbit or goat anti-mouse) labeled with horseradish peroxidase was added and incubated at 37 °C for 30~40 min and then washed with PBS for 3 times, 5~10 min each time; the sections were developed with 0.05% DAB-0.01% H_2O_2 for 2~10 min and then washed with PBS for 3 times, 5 min each time; the hematoxylin was added to counterstain the tissues for 20 s and then washed with water; the sections were dehydrated with gradient alcohol, and transparendized with xylene, and sealed with neutral gum in the end. The sections were observed under microscope and photographed with a pathological section scanner.

The stained protein signals in normal human skin tissues were used as positive controls, and the staining signals of replacing primary antibodies with PBS in normal human skin tissues were used as negative controls. The staining signals were considered to be positive if brown particles were present in the cytoplasm or nucleus (p63 protein was stained in the nucleus, and others were stained in the cytoplasm).

The staining signals of each protein between HHD patients and normal controls were examined and compared.

Real time-PCR

Total RNA was extracted and cDNA was synthesized according to the kit instructions. The primers were synthesized by Beijing Aoke Dingsheng Biotechnology Co., Ltd. according to the following sequences. MirNA-203: Forward 5'- ttgagttagggttatttttgtgt -3 '; Reverse 5'-ctaacccaaccaatttttccaa -3'. The PCR reaction: 2 × Taq Master Mix, 10 μl; cDNA, 2 μl; forward primer; 0.2 μl; reverse primer, 0.2 μl; DEPC water, 7.4 μl; total volume, 20 μl. PCR protocol: pre-denaturation, 95 °C, 3 min; denaturation, 95 °C, 12 s; annealing, 62 °C, 35 s; extension, 74 °C, 3 s; 40 cycles; extension, 74 °C, 5 min. The expression level of each gene was determined by relative quantification, and GAPDH included in the kit was used as an endogenous control. The relative expression level was determined by using the Ct value. Relative expression level = $2^{-\triangle\triangle CT}$.

Results

Pedigree analysis and clinical data of familial benign chronic pemphigus

1) Pedigree analysis and clinical data of pedigree Ⅰ
Among 4 generations of the pedigree, there are 2 HHD patients (1 male and 1 female) who were present in the 2nd and 3rd generations, consistent with the inheritance pattern of autosomal dominant genetic disease (Figure S1A).

The proband is a 50 year-old woman whose parents were not blood related. This patient was dianogsized at 28 years old. Physical exam showed that she had good health condition in general, and no abnormality was found in other body systems. Clinical manifestations included erythema, blisters, erosions under bilateral axilla, left groin and umbilicus, and slight hypertrophy of skin in the left groin (Figure S1B). Histopathological examination of typical skin lesions in the left groin revealed cracks in the epidermis and partial loss of the stratum corneum. The spines in the lower and middle layers of epidermis were loosened and cells of spinous layer were visible (Figure S1C).

2) Pedigree analysis and clinical data of family Ⅱ
Among 3 generations of the pedigree, there were 3 patients, one male and two female. The patients were present in two consecutive generations Ⅰ and Ⅱ, consistent with the inheritance pattern of autosomal dominant genetic disease (Figure S1D).

The proband was a 43 year-old male whose parents were not blood related. This patient was dianogsized at 33 years old. Physical exam showed that he had good general health condition without abnormality found in other body system. Clinical manifestations included flaky erythematous papule under the left

armpit and left groin, perianal area, left popliteal fossa, adjacent popliteal fossa, obvious erosion in addition to some erythema (Figure S1E). The left axillary skin lesions were taken for pathological examination. The results showed that the spines in the lower and middle layers of epidermis were loosened, and were overflowed on the top with red blood cells. A single layer of basal cells covered on the dermal papilla and formed a villi (Figure S1F).

3) Pedigree analysis and clinical data of sporadic case I
Among 3 generations of the pedigree, there was only 1 patient. No other patients in the pedigree were seen. No obvious sign of familial genetic disease was observed.

The patient was a 68 year-old male whose parents were not blood related. He was diagnosized at 36 years old. Physical exam showed that this patient was genereally in a good health condtion without obviousl abnormalities found in other body systems. Clinical manifestations included erythema on both sides of the groin and anus, scattered papules in addition to the anal erythema, obvious erosion and exudation in the skin lesions (Figure S2A). A piece of skin from lesions on the left groin was taken for histological exam. The results showed that spines in the middle and lower layers of the epidermis were loosen and formed fissures in which loosening cells were presented (Figure S2B).

4) Pedigree analysis and clinical data of sporadic cases ⵏ
Among 3 generations of the pedigree, there was 1 patient only. No other patients in the pedigree were seen. No obvious inheritance pattern of familial genetic diseases was shown.

The patient was a 42 years old male whose parents were not blood related. He was diagnosized at 31 years old. Physical exam showed that this patient had good general health condtion without other abnormalities found in other body systems. Clinical manifestations included slight erythema and desquamation on the back of right ear, erythematous papular rash on both sides of the groin, obvious erosion and exudation in addition to some erythema, and epidermal lesions on the left groin covered with crust (Figure S2C). Histopathological examination of the typical skin lesions from the left groin showed that the spinal layer in the epidermis formed fissures in which the loosening cells were scattered around (Figure S2D).

Gene sequencing of *ATP2C1*

1) PCR amplification for the exons of ATP2C1
Exon 26 of ATP2C1 in pedigree ⵏ, exon 15 of ATP2C1 in pedigree ⵏ, exon 8 of ATP2C1 in sporadic patient I, and exon 22 of ATP2C1 in sporadic patient ⵏ were amplified (Figure 1A). The sizes of PCR products were 312 bp, 383 bp, 425 bp and 298 bp respectively.

2) The sequencing result of exon 26 of ATP2C1 in pedigree I
A synonymous mutation c.G2598A in exon 26 was found in the proband of pedigree ⵏ, which was further confirmed by reverse sequencing that showed a complementary nucleotide mutation. The mutation did

not change amino acid code of lysine. We further verified this mutation was actually a nonsense mutation that was not previously reported (Figure 1B). Such mutation was not found in the normal members of this pedigree or other people who were not blood related (Figure 1C, D).

3) Sequencing results of ATP2C1 exon 15 in pedigree Ⅱ
A missense mutation c.C1286A was detected in the exon 15 of the proband in pedigree Ⅱ, which was further confirmed by reverse sequencing that showed a complementary nucleotide mutation. This mutation changed the original alanine to aspartic acid (p.A429D). We further verified that it was actually an unreported missense mutation (Figure 2A-D). Such mutation was not found in the normal members of this pedigree or other people who were not blood related (Figure 2B, C).

4) Sequencing results of ATP2C1 exon 8 in sporadic case Ⅰ
A nonsense mutation c.C635A in exon 8 was detected in the proband of sporadic case I. This mutation was further confirmed by reverse sequencing that showed a complementary nucleotide mutation. This mutation resulted in a premature stop codon in the polypeptide chain and was previously reported (Figures 3A-D). Such mutation was not seen in the normal human controls (Figure 3B, C).

5) Sequencing results of ATP2C1 exon 22 in sporadic case II
A missense mutation c. A1931G was detected in exon 22 of the proband in sporadic case Ⅱ, which was further confirmed by reverse sequencing that showed a complementary nucleotide mutation. This mutation changed the original 644th aspartic acid (GAU) to be Glycine (GGU) (p. D644G). We noticed that this mutation was previously reported (Figure 4A-D). Such mutation in the gene was not found in the normal members in the pedigree and other people who were not blood related (Figure 4B, C).

IHC staining for hSPCA1

hSPCA1 is mainly expressed in the cytoplasm of keratinocytes in the epidermal layer with some on the cell membrane. Positive staining appreaed as yellow or tan particles or clumps. In normal human skin tissues (Figure 5A-a), hSPCA1showed strong positive signals, that is, a dark brown stained band in the epidermis. The negative control in which the hSPCA antibody was replaced with PBS (Figure 5A-a, right corner inset) did not show any nonspecific staining. The expression levels of hSPCA1 in the skin tissues of all patients with HHD (Figure 5A-b/c/d) were significantly lower than that of the positive control, especially at the typical skin lesions (acanthosis). No obvious staining signal was seen even in some local areas (Figure. 5A-c).

IHC staining for proteins in relevant signaling pathways

1) IHC for p63
P63 is an intranuclear protein and can be stained in the nucleus of keratinocytes in the epidermal layer. In normal human skin tissues, p63 staining was strongly positive in the nucleus. In the area adjacent to the stratum corneum the nucleus gradually disappeared with differentiation, therefore, the staining is mainly present in the basal layer (Figure 5B-a). PBS was used as a negative control, which did not show any non-

specific staining (Figure 5B-a, right corner inset). The expression level of p63 protein in the nucleus of HHD patients was significantly reduced compared to the positive control, especially in the typical lesions (Figure 5B-b/c/d). No obvious staining was seen in some local areas of the tissue.

2) IHC for Notch1
Notch1 is expressed in the cytoplasm of keratinocytes in the epidermal layer. In normal human skin tissues, Notch1 was strongly stained, appeared as brown or tan particles or clumps (Figure 5C-a). In the entire epidermal layer, Notch1 showed a even deep-stained band. In the skin tissues of all HHD patients, Notch1 signals (Figure. 5C-b/c/d) were weaker compared to the positive control. In contrast, the negative control by using PBS instead of Notch1 antibody did not show any non-specific staining (Figure 5C-a, right corner inset).

3) IHC for HK□ protein
HK□ is expressed in the cytoplasm of the keratinocytes in the epidermal layer. In normal human skin tissues, HK□ was strongly stained (Figure 5D-a) and showed a even deep-stained band in the entire epidermal layer. In contrast, the expression level of HK□ in the cytoplasm of skin lesion tissues was significantly reduced compared to the normal human positive control (Figure 5D-b/c/d). The negative control by using PBS other than HK□ antibody (Figure 5D-a, right corner inset) did not show obviuos non-specific staining.

Real time PCR for Mir-203
RNA was extracted from the skin lesion tissues of HHD patients and real-time PCR was performed to detect the expression level of Mir-203 in these tissues. Normal human skin tissue was used as a control. The data showed that the levels of Mir-203 in the skin lesions of HHD patients were significantly upregulated compared to that in the normal human control (Figure 6).

Discussion

In this study, all patients (including all pedigree cases and sporadic cases) we collected have typical clinical manifestations and histopathological characteristics. Pedigree I and pedigree II showed vertical transmission and presented in an inheritance pattern of autosomal dominant genetic disease. By using gene sequencing and exon alignment of ATP2C1 from 4 patients, we found 4 different heterozygous mutations, including 1 synonymous mutation c.G2598A, 2 missense mutations c.C1286A and c. A1931G, and 1 nonsense mutation c.C635A.

We then searched in Gene Bank gene database and UniProt protein resource database for confirmed mutations in the gene ATP2C1 and further analyzed the mutations we found. In the patient of pedigree I, the synonymous mutation c.G2598A in exon 26 changed the codon from AAG to AAA, but did not change the amino acid (lysine). In the patient of pedigree II, the missense mutation c.C1286A (p.A429D) in exon 15 changed the alanine to aspartic acid. Protein structural analysis showed that this mutation was located in the P region (phosphorylation region), the most important functional site of hSPCA1 to which

Ca^{2+}/Mn^{2+} and ATP are bound. This mutation changed the primary structure of the protein and disrupted the catalytic site of ATPase, phosphorylation function and protein conformation, leading to loss of protein function and transport failure of Ca^{2+}/Mn^{2+} and abnormal concentrations of intracellular Ca^{2+}/Mn^{2+} in the cells.

In keratinocytes, hSPCA1 not only transports Ca^{2+}, but also competitively transports one Mn^{2+} from the cytoplasm to the Golgi apparatus, which is nonreplacible by other calcium pumps. It is known that the cells are very sensitive to Mn^{2+} concentration and a slight change of Mn^{2+} concentration may affect cell metabolism seriously[29]. Excessive intracellular Mn^{2+} may prevent Mg^{2+} binding to proteins, compromise the fidelity of DNA polymerase, and disrupt the transport function of cell membranes, thus affecting the physiological conditions of human body[30, 31]. In sporadic case I, a nonsense mutation c.C635A in exon 8 changed the serine codon UCG (position 212) to a stop codon UAG. This mutation is located in the A region of regulatory element and results in premature polypeptide chain. In addition, the mRNA with this nonsense mutation is easily degraded, reducing the expression level of truncated hSPCA1 that lacks important structures in the calcium pump. In sporadic case Ⅱ, a missense mutation c. A1931G in exon 22 changed aspartate (GAU, at position 644) to glycine (GGU) (p. D644G). This mutation is located at the Mn^{2+} binding site of hSPCA1[32] and disrupts the binding of hSPCA1 to Mn^{2+}, thus interfere the metabolism of intracellular Mn^{2+} [33], affect the activity of DNA polymerase and the transport function of cell membranes, and increase the potential of mutation in other genes [31].

hSPCA1 is highly expressed in the skin and kidney tissues, localized in cytoplasmic Golgi apparatus in the cells. The clinical symptoms of ATP2C1 mutation are mainly limited to the skin of the patients. Therefore, we chose skin lesions to investigate dysregulated signaling pathways in HHD patients. Immunohistochemistry data showed that the expression levels of hSPCA1 in the skin tissues of all HHD patients was significantly downregulated compared to normal human controls.

The tumor suppressor Mir-203 is specifically expressed in keratinocytes and is sensitive to changes of intracellular Ca^{2+} concentration. In the keratinocytes of HHD patients, Ca^{2+} concentration is strikingly increased due to the dysfunction of the calcium pump. In our study, Mir-203 in the skin lesions of patients showed a significant upregulation. p63 is highly expressed in basal cells and plays an important role in the proliferation and differentiation of keratinocytes[19]. Immunohistochemical staining and the quantification graph showed that p63 is significantly downregulated compared to the normal human controls. From previous studies and ours, it is belived that increased intracellular Ca^{2+} concentration is actually accompanied by upregulation of Mir-203 and downregulation of p63. We also found that the expression level of Notch1, which is negatively regulated by p63, only showed a slight decrease. In this study, our data suggest that p63 and Mir-203 are both associated with Notch1 in the skin lesions.

HK is one of the key enzymes for glycolysis in the skin and is also a target gene of p63. Downregulation of HK directly reduces ATP production[20], which in turn inhibits hSPCA1 function that is very much dependent on energy supply. From HK IHC and the quantification chart, it was shown that the level of

HKⅡ in the tissues of HHD patients was obviously decreased to about 60% of the normal value. Our data demonstrate that increased Ca^{2+} concentration caused by ATP2C1 mutation does result in decreased HKⅡ, which reduces ATP production and affects normal physiological function of the human body.

Conclusion

In this study, we detected novel ATP2C1 mutations in HHD patients, which has further enriched the pathogenic mutation pool of HHD. Our work is not only helpful for further diagnosis of the disease at the molecular level, but also helpful for the understanding of ATP2C1 mutations and HHD pathogenesis. We showed that Mir-203 was upregulated in HHD patients, which in turn might downregulate p63 and Notch1, and downregulation of p63 might further decrease the level of HKⅡ, leading to defective energy production and disabled cell adhesion. This regulatory cascades might contribute to the pathogenesis of HHD. We also noticed that Mir-203, p63 and other factors in the signaling pathways all interact with other factors and form a regulatory network, indicating that there are multiple signaling pathways contributing to HHD. The exact mechanism underlying HHD pathogenesis remains unclear and needs further inverstigation.

Abbreviations

HHD
Hailey-Hailey disease; hSPCA1:human secretory pathway Ca^{2+}/Mn^{2+} -ATPase protein 1; HE:hematoxylin-eosin; PCR:polymerase chain reaction.

Declarations

Acknowledgements

Not applicable.

Consent to publish

The patient's legal guardians (parents) have provided written consent to publish this case report, including medical data and images.

Authors' contributions

Xiaoli Li wrote the main manuscript text, Dingwei Zhang prepared Figures. Jiahui Ding and Li Li were responsible for the patient's clinical and surgical management. Zhenghui Wang reviewed the manuscript and contributed to the paper organization. All authors read and approved the final manuscript.

Funding

Not applicable.

Availability of data and materials

For further details regarding this paper, please contact Prof Zhenghui Wang ,PhD

Ethics approval and consent to participate

The patient was studied as part of a research protocol approved by the Ethics Committee of The Second Affiliated Hospital, Xi'an Jiaotong University(2015-038). The patient's legal guardians (parents) have signed informed consent to participate in this study.

Competing interests

The authors declare that they have no competing interests.

References

1.
Chao SC, Tsai YM, Yang MH. Mutation analysis of ATP2C1 gene in Taiwanese patients with Hailey-Hailey disease. Br J Dermatol. 2002;146:595–600.
2.
Cheng Y, Cheng YM, Zhao G, Jia MC. A novel missense mutation of the ATP2C1 gene in a Chinese patient with Hailey-Hailey disease. Bioch Biophy Res Commun. 2011;406:420–2.
3.
Voisset C, Garcia-Rodriguez N, Birkmire A, Blondel M, Wellinger RE. Using yeast to model calcium-related diseases: example of the Hailey-Hailey disease. Biochem Biophys Acta. 2014;1843:2315–21.
4.
Burge SM. Hailey-Hailey disease: the clinical features, response to treatment and prognosis. British J Dermato. 1992;126:275–82.
5.
Le Sache-de Peufeilhoux L, Raynaud E, Bouchardeau A, Fraitag S, Bodemer C. Familial benign chronic pemphigus and doxycycline: a review of 6 cases. J Eur Acad Dermato Vener: JEADV. 2014;28:370–3.
6.
Almeida L, Grossman ME. Benign familial pemphigus complicated by herpes simplex virus. Cutis. 1989;44:261–2.
7.
Ikeda S, Suga Y, Ogawa H. Successful management of Hailey-Hailey disease with potent topical steroid ointment. J Dermatol Sci. 1993;5:205–11.
8.
Jeon SY, Ha SM, Ko DY, Song KH, Kim KH. Hailey-hailey disease treated with topical tacalcitol. Ann Dermatol. 2013;25:389–90.
9.

Rajpara SM, King CM. Hailey-Hailey disease responsive to topical calcitriol. Bri J Dermatol. 2005;152:816–7.

10.

Vanderbeck KA, Giroux L, Murugan NJ, Karbowski LM. Combined therapeutic use of oral alitretinoin and narrowband ultraviolet-B therapy in the treatment of hailey-hailey disease. Dermatol Rep. 2014;6:5604.

11.

Norman R, Greenberg RG, Jackson JM. Case reports of etanercept in inflammatory dermatoses. J Am Acad Dermatol. 2006;54:139–42.

12.

Micaroni M, Giacchetti G, Plebani R, Xiao GG, Federici L. ATP2C1 gene mutations in Hailey-Hailey disease and possible roles of SPCA1 isoforms in membrane trafficking. Cell Death Dis. 2016;7:e2259.

13.

Holst VA, Fair KP, Wilson BB, Patterson JW. Squamous cell carcinoma arising in Hailey-Hailey disease. J Am Acad Dermatol. 2000;43:368–71.

14.

Cockayne SE, Rassl DM, Thomas SE. Squamous cell carcinoma arising in Hailey-Hailey disease of the vulva. Br J Dermato. 2000;142:540–2.

15.

Chun SI, Whang KC, Su WP. Squamous cell carcinoma arising in Hailey-Hailey disease. J Cutan Pathol. 1988;15:234–7.

16.

Wang K, Zhang ZW. Expression of miR-203 is decreased and associated with the prognosis of melanoma patients. Int J Clin Exp Pathol. 2015;8:13249–54.

17.

Hildebrand J, Rutze M, Walz N, Gallinat S, Wenck H, Deppert W, et al. A comprehensive analysis of microRNA expression during human keratinocyte differentiation in vitro and in vivo. J Invest Dermatol. 2011;131:20–9.

18.

Nguyen BC, Lefort K, Mandinova A, Antonini D, Devgan V, Della Gatta G, et al. Cross-regulation between Notch and p63 in keratinocyte commitment to differentiation. Genes Develop. 2006;20:1028–42.

19.

Wu N, Rollin J, Masse I, Lamartine J, Gidrol X. p63 regulates human keratinocyte proliferation via MYC-regulated gene network and differentiation commitment through cell adhesion-related gene network. J Bio Chem. 2012;287:5627–38.

20.

Viticchie G, Agostini M, Lena AM, Mancini M, Zhou H, Zolla L, et al. p63 supports aerobic respiration through hexokinase II. P Natl Acad Sci USA. 2015;112:11577–82.

21.

Truong AB, Kretz M, Ridky TW, Kimmel R, Khavari PA. p63 regulates proliferation and differentiation of developmentally mature keratinocytes. Genes Develop. 2006;20:3185–97.

22.

McDade SS, Patel D, McCance DJ. p63 maintains keratinocyte proliferative capacity through regulation of Skp2-p130 levels. J Cell Sci. 2011;124:1635–43.

23.

Ma J, Meng Y, Kwiatkowski DJ, Chen X, Peng H, Sun Q, et al. Mammalian target of rapamycin regulates murine and human cell differentiation through STAT3/p63/Jagged/Notch cascade. J Clin Invest. 2010;120:103–14.

24.

Lena AM, Shalom-Feuerstein R, Rivetti di Val Cervo P, Aberdam D, Knight RA, Melino G, et al. miR-203 represses 'stemness' by repressing DeltaNp63. Cell Death Differ. 2008;15:1187–95.

25.

Yi R, Poy MN, Stoffel M, Fuchs E. A skin microRNA promotes differentiation by repressing 'stemness'. Nature. 2008;452:225–9.

26.

Sasaki Y, Ishida S, Morimoto I, Yamashita T, Kojima T, Kihara C, et al. The p53 family member genes are involved in the Notch signal pathway. J Bio Chem. 2002;277:719–24.

27.

Kopan R, Ilagan MX. The canonical Notch signaling pathway: unfolding the activation mechanism. Cell. 2009;137:216–33.

28.

Gao S, Chen X, Jin H, Ren S, Liu Z, Fang X, et al. Overexpression of ErbB2 renders breast cancer cells susceptible to 3-BrPA through the increased dissociation of hexokinase II from mitochondrial outer membrane. Oncol Lett. 2016;11:1567–73.

29.

Towler MC, Prescott AR, James J, Lucocq JM, Ponnambalam S. The manganese cation disrupts membrane dynamics along the secretory pathway. Exp Cell Res. 2000;259:167–79.

30.

Monk S, Sakuntabhai A, Carter SA, Bryce SD, Cox R, Harrington L, et al. Refined genetic mapping of the darier locus to a < 1-cM region of chromosome 12q24.1, and construction of a complete, high-resolution P1 artificial chromosome/bacterial artificial chromosome contig of the critical region. Am J Human Gene. 1998;62:890–903.

31.

Behne MJ, Tu CL, Aronchik I, Epstein E, Bench G, Bikle DD, et al. Human keratinocyte ATP2C1 localizes to the Golgi and controls Golgi Ca^{2+} stores. J Invest Dermatol. 2003;121:688–94.

32.

Brini M, Carafoli E. Calcium pumps in health and disease. Physiol Rev. 2009;89:1341–78.

33.

Foggia L, Aronchik I, Aberg K, Brown B, Hovnanian A, Mauro TM. Activity of the hSPCA1 Golgi Ca^{2+} pump is essential for Ca^{2+}-mediated Ca^{2+} response and cell viability in Darier disease. J Cell Sci. 2006;119:671–9.

Table 1

Table 1. PCR protocol

	94 °C 5 min				
⬜	94 °C 45s	60°C 45s	72°C 45s	2×	1
	94 °C 45s	59°C 45s	72°C 45s	2×	
	94 °C 45s	58°C 45s	72°C 45s	2×	
	94 °C 45s	57°C 45s	72°C 45s	2×	
	94 °C 45s	56°C 45s	72°C 45s	2×	
	94 °C 45s	55°C 45s	72°C 45s	20×	
⬜	94 °C 45s	55°C 45s	72°C 45s	32×	Other exon
⬜	94 °C 30s	54°C 30s	72°C 30s	30×	5, 7, 12, 27, 28

Figures
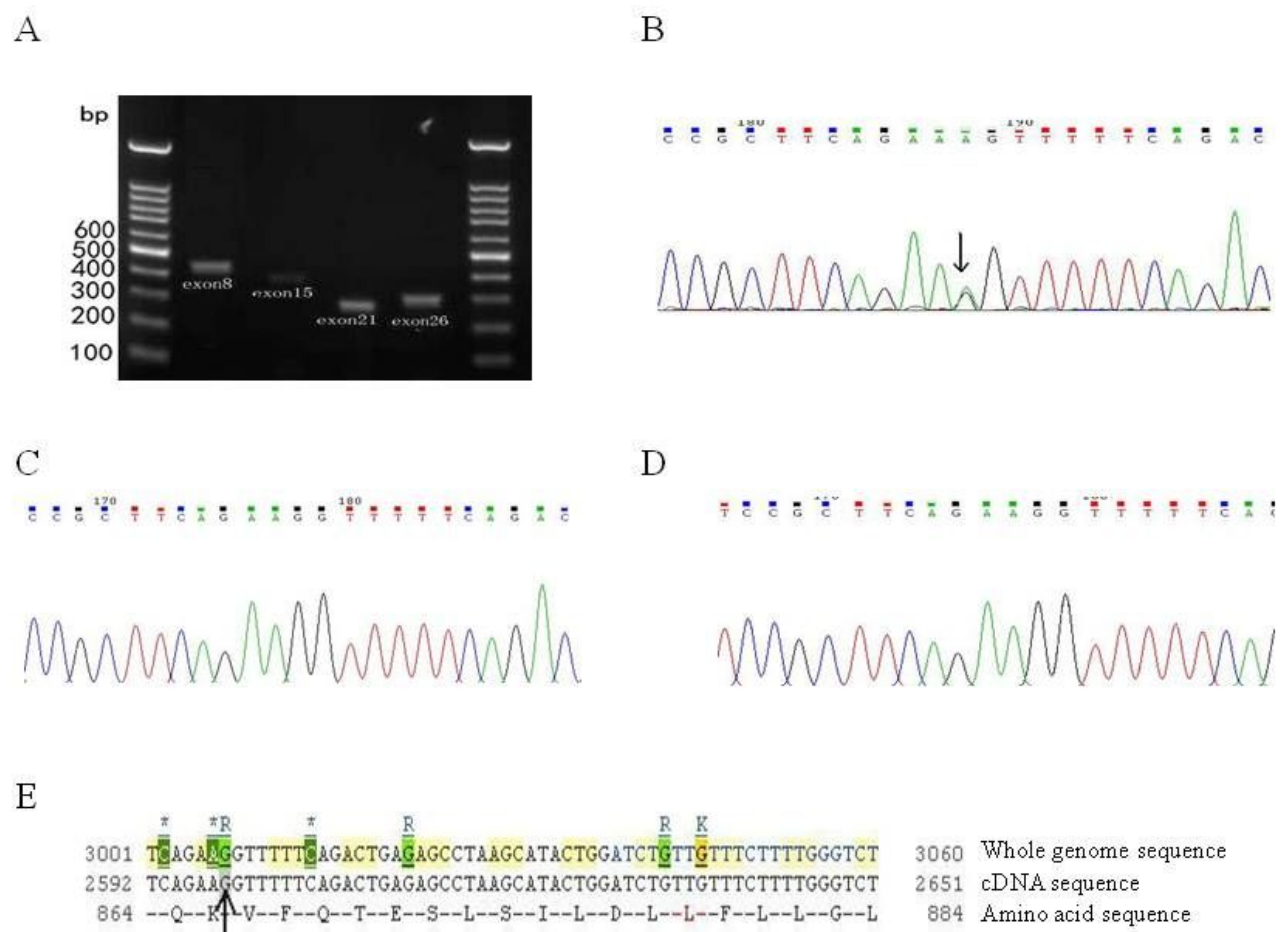
Figure 1

Exon 26 sequencing for the ATP2C1 gene in pedigree Ⅰ (A) PCR amplification for exons 8, 15, 22 and 26 of ATP2C1. (B). Sequencing result of exon 26 for the proband in pedigree I. (C). Sequencing result of exon 26 for normal member in the same pedigree. (D). Sequencing result of exon 26 for normal individual who was not blood related. (E). Mutation in exon 26 of ATP2C1 gene in the Ensemble database (indicated by arrows).
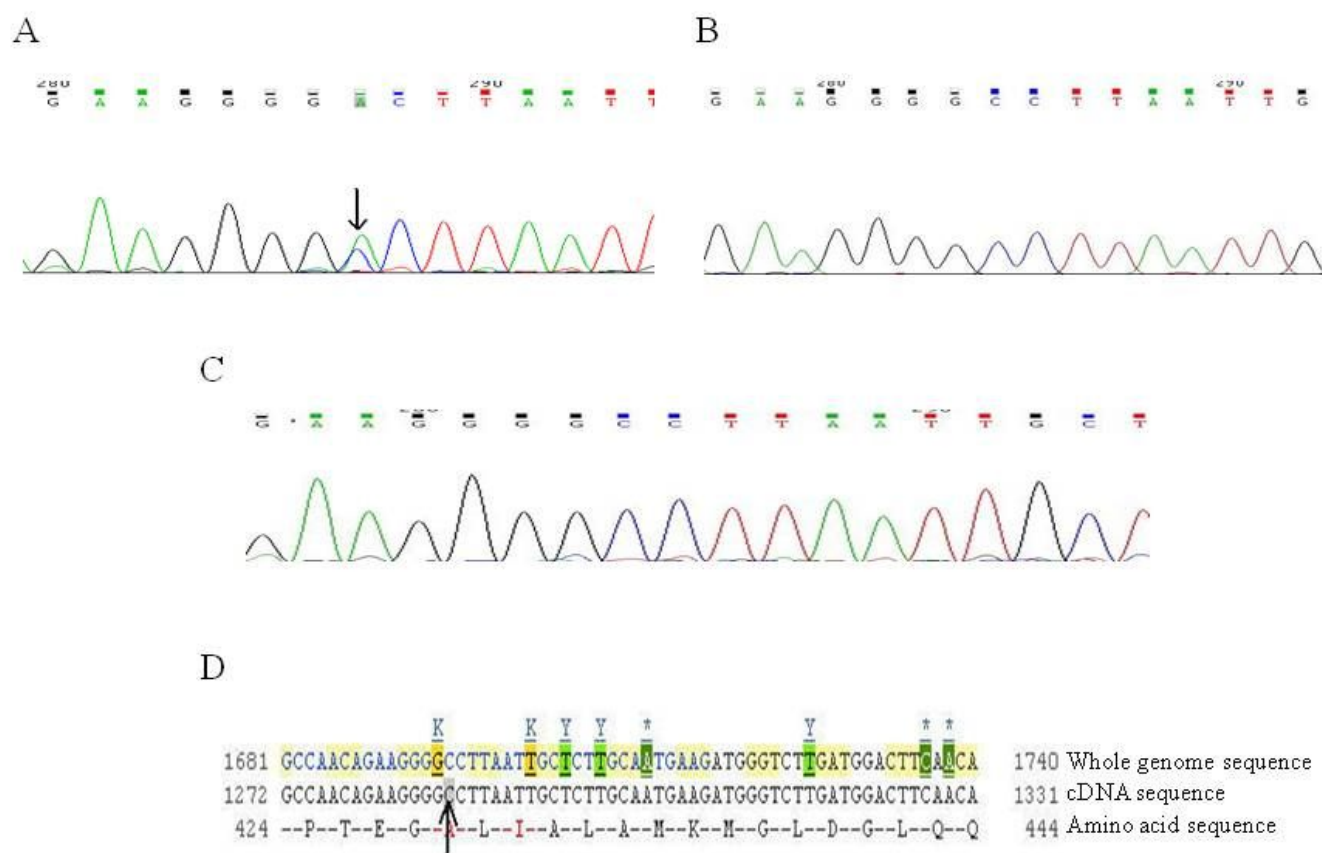
Figure 2

Exon 15 sequencing for the ATP2C1 gene in pedigree II (A). Sequencing result of exon 15 for the proband in pedigree II. (B). Sequencing result of exon 15 for normal member in the same pedigree. (C). Sequencing result of exon 15 for normal individual who was not blood related. (D). Mutation in exon 15 of ATP2C1 gene in the Ensemble database (indicated by arrows).
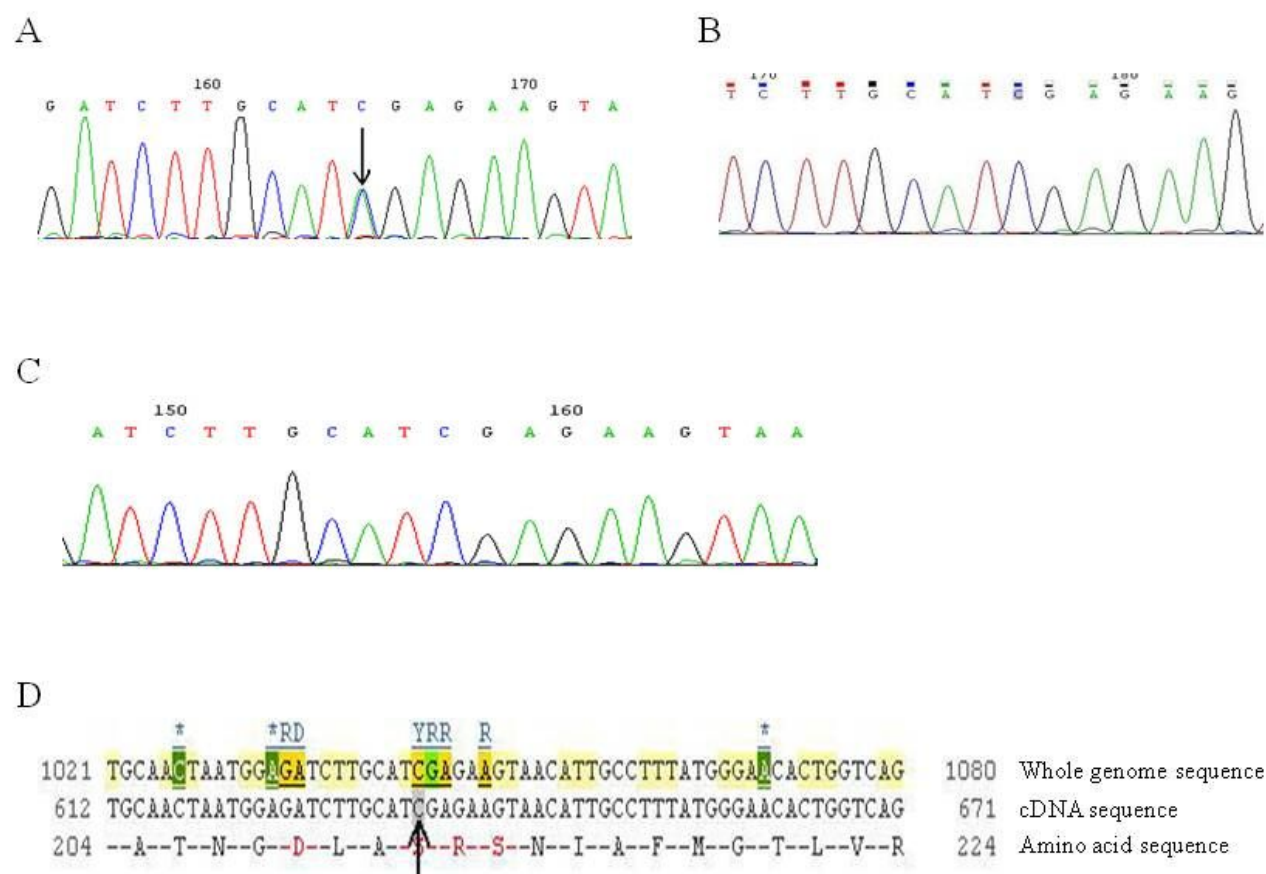
Figure 3

Exon 8 sequencing for the ATP2C1 gene in sporadic case I (A). Sequencing result of exon 8 in sporadic case I. (B). Sequencing result of exon 8 for normal member in the same pedigree. (C). Sequencing result of exon 8 for normal individual who was not blood related. (D). Mutation sites in exon 8 of ATP2C1 gene in the Ensemble database (indicated by arrows).
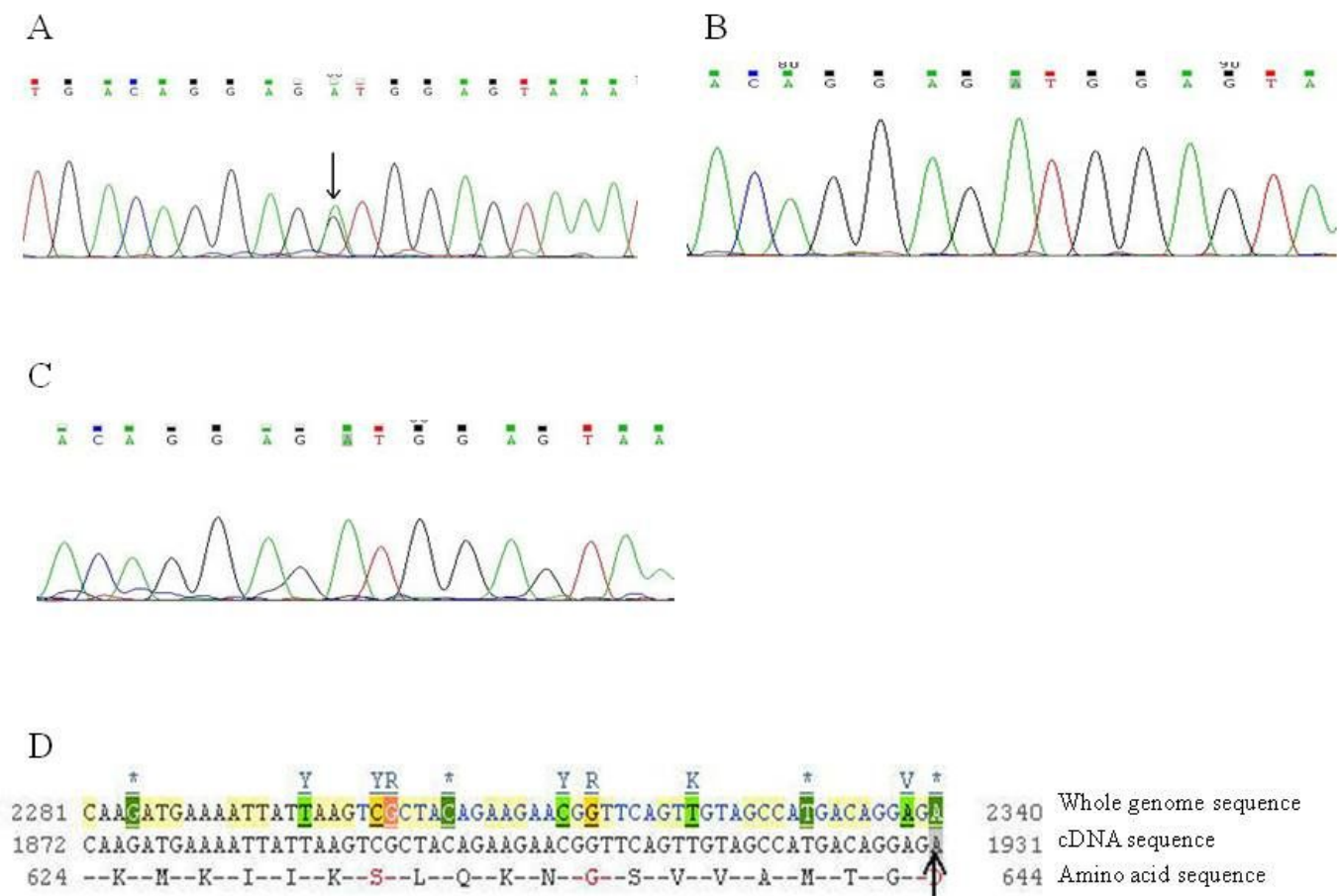
Figure 4

Exon 22 sequencing for the ATP2C1 gene in sporadic case II (A). Sequencing result of exon 22 in sporadic case II. (B). Sequencing result of exon 22 for normal member in the same pedigree. (C). Sequencing result of exon 22 for normal individual without blood relation. (D). Mutation sites in exon 22 of ATP2C1 gene in the Ensemble database (indicated by arrows).
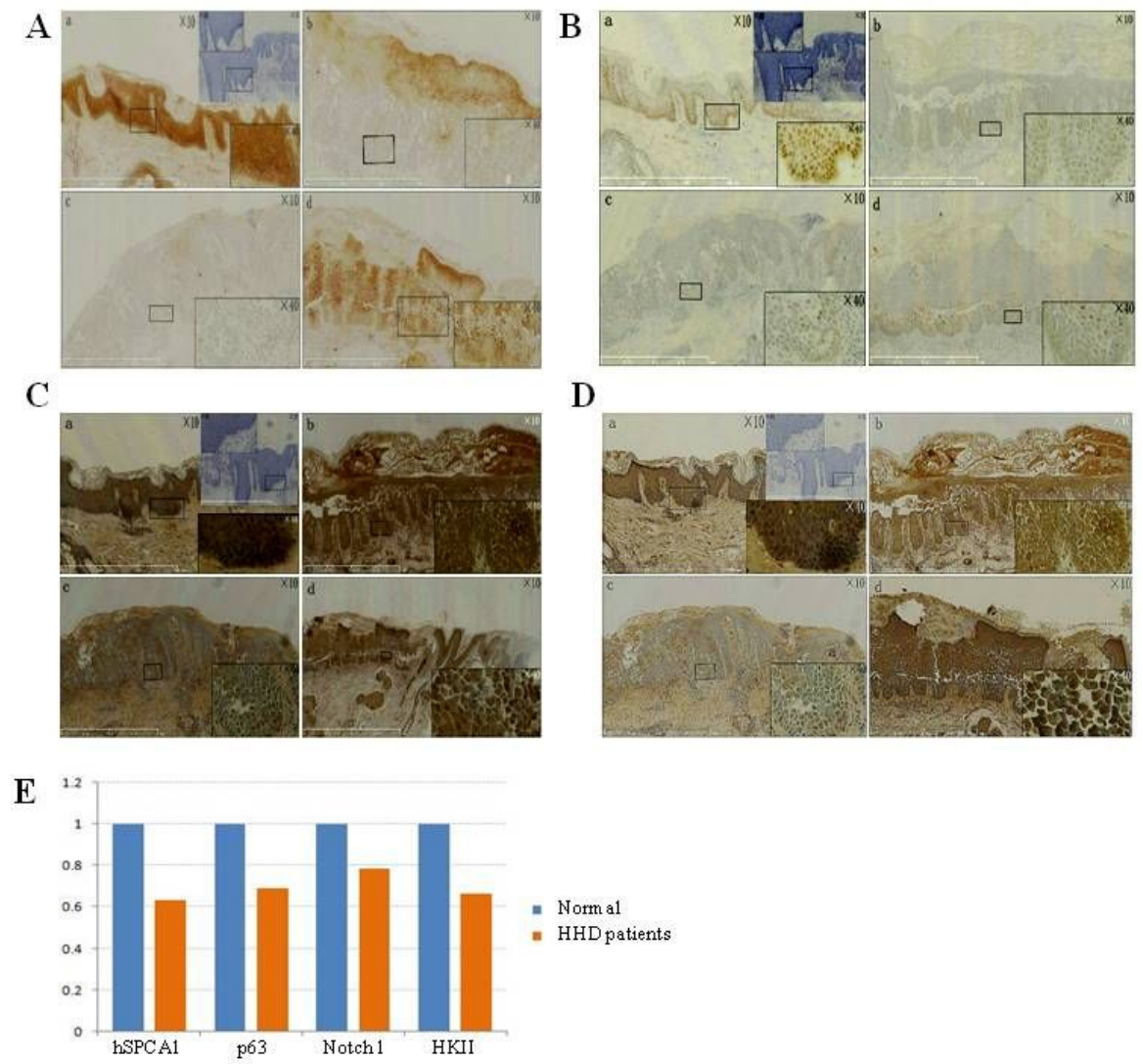
Figure 5

(A). IHC staining for ATP2C1. (B). IHC staining for p63. (C). IHC staining for Notch I. (D). IHC staining for HKII. (E). Quantification for IHC staining signals in A~D.
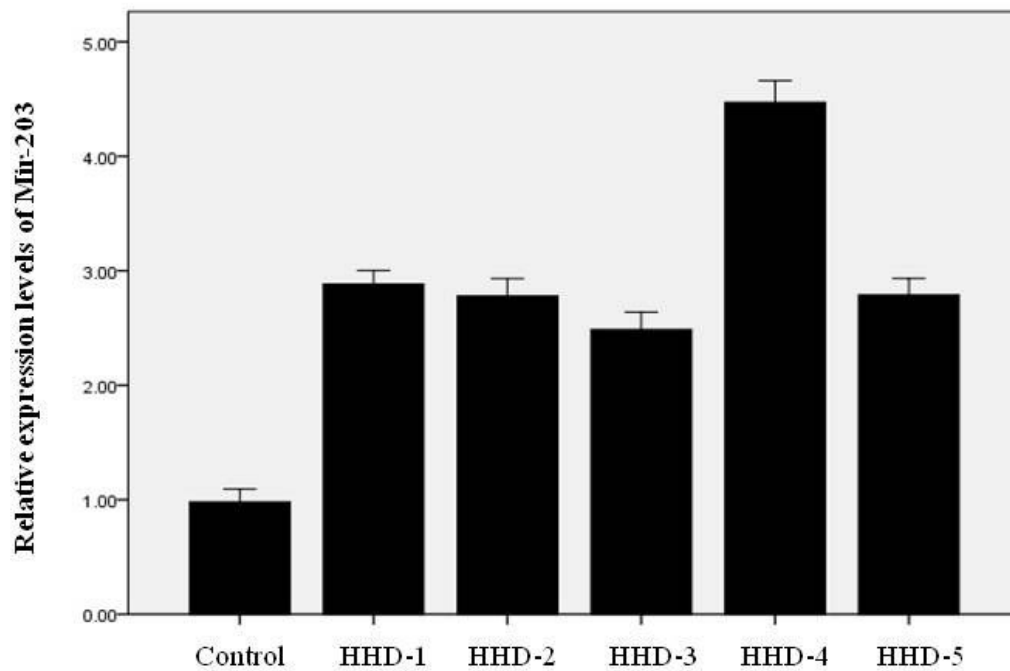
Figure 6

Mir-203 expression in HHD patients. Real-time PCR was performed to examine the expression levels of Mir-203 in HHD patients.